construction materials

MDPI

Article

Durability of One-Part Alkali-Activated Binder Made with Alternative Sodium Silicate

Rodrigo H. Geraldo [1], Jardel P. Gonçalves [2] and Gladis Camarini [3,*]

[1] Civil Engineering Department, FACENS University, Campus Alexandre Beldi Netto, Rodovia Senador José Ermírio de Moraes, 1425, Castelinho km 1.5, Alto da Boa Vista, Sorocaba 18087-125, São Paulo, Brazil; rodrigoh.geraldo@gmail.com

[2] Polytechnic School, Centro Interdisciplinar de Energia e Ambiente (CIENAM), Bahia Federal University (UFBA), Campus da Federação, Rua Aristides Novis, 02, Salvador 40210-630, Bahia, Brazil; jardelpg@gmail.com

[3] Civil Engineering Department, School of Engineering of Guaratingueta, São Paulo State University (UNESP), Campus FEG (Guaratinguetá), Av. Dr. Ariberto Pereira da Cunha, 333-Pedregulho, Guaratinguetá 12516-410, São Paulo, Brazil

* Correspondence: gcamarini@gmail.com

Abstract

Recent studies have highlighted the potential for production of an alternative sodium silicate in powder obtained by mixing NaOH with rice husk ash, followed by a dissolution and drying process. This alternative sodium silicate, when mixed with metakaolin and dried under special conditions, results in an eco-friendly one-part alkali-activated binder (OPAAB). However, the durability performance of OPAAB incorporating RHA-derived sodium silicate remains largely unexplored. This study focuses on an experimental investigation of OPAAB mortar durability, analyzing permeability, high-temperature exposure, wet-and-dry cycles, and resistance to aggressive environments (sulfate and acid attack). A two-part mix mortar made with the same precursors was used as a reference. It was found that the OPAAB mortars were not affected by the wet-and-dry cycles nor the sulfate attack. Exposure to high temperature (900 °C for 1 h) did not cause specimen failure, which had a residual compressive strength higher than 5 MPa. Finally, exposure to sulfuric acid for 56 days decreased the mechanical strength of the mortars, but all the specimens maintained a residual compressive strength higher than 4 MPa. The durability performance of the mortars produced with OPAAB incorporating RHA-derived sodium silicate was similar to the two-part mix mortars (reference), demonstrating technical feasibility and advancing the understanding of durability aspects for application in civil construction.

Keywords: alternative sodium silicate; acid attack; sulfate attack; fire resistance; permeability; durability

Check for updates

Received: 23 December 2025
Revised: 10 January 2026
Accepted: 20 January 2026
Published: 28 January 2026

Copyright: © 2026 by the authors. Licensee MDPI, Basel, Switzerland. This article is an open access article distributed under the terms and conditions of the Creative Commons Attribution (CC BY) license.

1. Introduction

Alkali-activated binder (AAB) is a material produced by a reaction between aluminosilicate materials and an alkali source, and it is seen as an environmentally friendly alternative to Portland cement (PC) [1,2]. Different authors have stated the potential of AAB and AAB-based materials to decrease carbon dioxide (CO_2) and other greenhouse gas (GHG) emissions compared to PC products (Table 1).

Table 1. Literature data on AAB reduction of CO_2 and other GHGs compared to PC.

CO_2 and Other GHG Reduction Rate [1]	Reference
80–90	Davidovits [3]
80	Khale and Chaudhary [4]
80	Duxson et al. [5]
73	Jiang et al. [6]
73	Robayo-Salazar et al. [7]
72.4	Borges et al. [8]
70	Weil et al. [9]
63	Mellado et al. [10]
62	Abdulkareem et al. [11]
55–75	Yang et al. [12]
55–75	Passuello et al. [13]
54	Carreño-Gallardo et al. [14]
45	Habert et al. [15]
44–64	McLellan et al. [16]
40	Heath et al. [17]
32–43	Teh et al. [18]
27–45	Nguyen et al. [19]
23–55	Maddalena et al. [20]
9	Turner and Collins [21]

[1] Some authors compared AAB concrete with PC concrete.

The data presented in Table 1 reveal that AAB has the potential to decrease CO_2 and other GHG emissions when compared to PC, even considering the most conservative result (9% reduction). The reduction rate changes with the raw materials employed, the local availability of precursors, transportation, use or not of thermal curing, and other factors [16,21]. Teh et al. [18] concluded that AAB-based concrete can reduce GHG emissions between 32 and 43% depending on the raw material used in its production when compared to PC-based concrete with the same compressive strength. Jiang et al. [6] also showed that AAB-based concrete emitted 73% less GHG and consumed less energy (43%) and less water (23%) when compared to conventional concrete with the same compressive strength.

According to the mix production, AAB can be classified as "two-part", when there is a liquid-based activator with solid aluminosilicate, or "one-part" when both precursors (activator and aluminosilicate sources) are solids [2].

The two-part method employs an activator solution based on the mixture of an alkaline source (e.g., potassium or sodium hydroxide) with water. For large-scale applications, the handling, transportation, and management of high-viscosity solutions have some challenges (e.g., high cost, injuries during the application, and contamination risks) [22,23].

One-part alkali-activated binder (OPAAB) was proposed to mitigate these disadvantages and allow a more extensive application of AAB [22], because the alkaline and alumino-silicate sources are mixed in powder form, resulting in a blend to which only water is added to initiate reactions, similar to PC [24]. This approach involves simply mixing the water into the dry blend precursors to initiate the reaction, enhancing the safety by eliminating the use of highly viscous alkaline solutions at the construction site, thereby increasing acceptance and commercialization potential [25–28].

The choice of precursors is very important to produce OPAABs that are commercially feasible and environmentally sustainable. Sodium silicate powder has been used to produce OPAABs with good properties for civil construction [29–32]. However, commercial sodium silicate causes the main environmental problem of AAB [19], and high energy consumption is necessary to produce sodium silicate powder, resulting in an OPAAB with lower environmental benefits compared to a two-part AAB [33].

The use of locally available raw materials allows low costs and low GHG emissions, and the use of chemically modified wastes to produce alternative activators expands the environmental performance of OPAAB [11].

One option to produce alternative solid alkali activators is the use of rice husk ash (RHA). RHA is an agricultural waste, and it is used as a fuel for electricity generation. This burning process results in the RHA, which represents around 18% of the fired shell initial volume. It is estimated that 1 ton of rice generates between 200 and 250 kg of rice husk, which, when burned, represents 36–45 kg of rice husk ash [34,35]. Therefore, the volume of RHA produced is considerable, making it essential to determine an environmentally friendly method of disposal.

Studies by Geraldo et al. [36,37] have introduced a method for producing OPAABs using alternative sodium silicate from RHA. The authors found that the process of dissolution of RHA into NaOH solution, with heating and mixing, followed by drying and milling, results in an alternative sodium silicate in powder with reactive characteristics. When this powder is mixed with metakaolin, it forms an OPAAB [36]. It was also concluded that with a proper mix design (e.g., using a more reactive metakaolin and decreasing the water content used to produce the fresh binder), it is possible to obtain mortars with mechanical strengths suitable for different applications in the construction industry (the authors stated a compressive strength higher than 35 MPa at 28 days) [37].

However, despite the promising mechanical strength results, the durability performance of eco-friendly OPAAB incorporating RHA-derived sodium silicate remains largely unexplored. Systematic durability assessments focusing on OPAAB formulations produced with alternative, waste-derived sodium silicate are still missing in the literature. Durability is a key parameter in determining the success and the acceptance of new construction materials, as it directly governs service life, maintenance demand, and environmental performance. Therefore, understanding the durability of OPAAB-based products is essential for their application, commercial viability, and large-scale adoption in the civil construction industry [5,38].

In this context, ensuring the durability of one-part alkali-activated binders (OPAABs) is essential not only for their structural reliability but also for their commercial viability and large-scale adoption. From a life-cycle assessment perspective, the environmental benefits associated with low-carbon binders can only be realized if adequate durability is achieved, as premature degradation would offset gains obtained during production. Therefore, validating the durability performance of OPAAB-based materials is a determining factor for their practical application, commercial development, and dissemination within the civil construction industry [5,38].

In this context, this research aims to study the durability properties of OPAAB mortars produced with alternative sodium silicate powder obtained from RHA dissolution. The work investigates the permeability properties, resistance to high temperature and wet–dry cycles, and the effects of acid and sulfate on OPAAB-based mortars. Their performances were compared with a two-part AAB-based mortar.

2. Materials and Methods

2.1. Materials

The alkali source used was sodium hydroxide (NaOH) flakes with 97.5% purity (Unipar Carbocloro S.A., Sao Paulo, Brazil). Two different metakaolins were tested as aluminosilicate sources: MK1 (metakaolin type 1) and MK2 (metakaolin type 2, more reactive). MK1 and MK2 were supplied by Metacaulim do Brasil Indústria e Comércio Ltd. (Jundiaí, São Paulo, Brazil), and MK2 is more reactive than MK1. RHA (Sílica Verde

do Arroz Ltd., Alegrete, Rio Grande do Sul, Brazil) was employed as a source of SiO_2 to produce the alternative sodium silicate.

The chemical compositions and physical properties of the solid precursors are presented in Table 2.

Table 2. Chemical compositions and physical properties of MK1, MK2, and RHA.

Oxides (Mass %)	MK1	MK2	RHA
SiO_2	49.36	51.30	93.19
Al_2O_3	41.07	43.48	1.27
K_2O	2.45	1.20	1.51
Fe_2O_3	2.08	0.51	0.05
TiO_2	1.40	0.03	-
MgO	0.82	0.11	0.33
CaO	0.07	0.04	0.58
Others	0.30	0.34	0.99
Loss on ignition	2.45	2.99	2.08
pH	6.00	6.08	9.94
Physical properties			
Specific mass (kg/m^3)	2775	2664	2388
Bulk density (kg/m^3)	439	422	479
$D_{10\%}$ (μm)	2.17	1.18	2.47
$D_{50\%}$ (μm)	11.32	6.15	13.83
$D_{90\%}$ (μm)	41.37	47.15	51.10

Table 2 indicates that MK2 exhibits a $D_{50\%}$ value nearly half that of MK1, evidencing its finer particle size distribution. RHA presents the highest $D_{50\%}$ and the lowest bulk density among the raw materials. The behavior of the final mixtures is associated with differences in the reactivity of both the metakaolin and the alkaline activator, which directly influence the resulting properties of the OPAAB. Previous studies have shown that MK2 displays higher reactivity than MK1, leading to increased formation of N–A–S–H gel. Consequently, it can generate the formation of networks that lead to microstructure variations, enhancing binder performance [37].

Natural sand was used as fine aggregate with a specific gravity of 2609 kg/m^3, bulk density of 1890 kg/m^3, fineness modulus of 2.38, and maximum particle size of 2.4 mm.

Water from the municipal supply was used in the mixtures.

2.2. OPAAB Production

The OPAAB was obtained through the method described by Geraldo et al. [36], which is briefly presented below.

RHA was mixed in NaOH solution using a mass ratio of 1 NaOH/1.605 water/1.284 RHA. The resulting slurry was kept in a magnetic stirrer (equipment: Fisatom 752A, Fisatom, São Paulo, São Paulo, Brazil) with heating (90 ± 5 °C). Due to the high viscosity of the mixture, mechanical stirring was applied using a mechanical stirrer (Fisatom 713D) equipped with a stainless steel stem and operated at 500–600 rpm. After 30 min of mixing, the slurry was collected and oven-dried in a stationary kiln with air circulation at a temperature of 200 ± 10 °C for 3 h.

After drying was complete, the material was collected, crushed using a porcelain ball mill with porcelain grinding balls, and sieved. The resulting material was sieved using a 0.075 mm mesh, and the alternative sodium silicate in powder was formed.

The powdered alternative sodium silicate was mixed with metakaolin (MK1 or MK2) to produce the OPAAB.

2.3. Mortar Production

Table 3 shows the identification of each mix design.

Table 3. Mortar mix designs.

Mortar	ASSP [6] (g)	NaOH (g)	MK1 (g)	MK2 (g)	RHA (g)	Sand (g)	Water (g)	SiO_2/Al_2O_3 (mol/mol)
M1(−R) [1]	42.0	-	80	0	3.6	244	71.80	3.3
M2(+R) [2]	42.0	-	0	80	3.6	244	71.80	3.1
M2-10 [3]	42.0	-	0	80	3.6	244	64.62	3.1
M2-20 [4]	42.0	-	0	80	3.6	244	57.44	3.1
TPM [5]	-	81	355	-	104	1065	230	4.2

[1] (−R) = Mortar made with MK1, lower reactivity. [2] (+R) = Mortar made with MK2, higher reactivity than MK1. [3] M2-10 = Similar to M2 (+R)[2], with reduction of 10% (weight mass) in water content. [4] M2-20 = Similar to M2 (+R)[2], with reduction of 20% (weight mass) in water content. [5] TPM = two-part mix (mortar produced with two-part mix AAB, used as a reference). [6] ASSP = Alternative sodium silicate in powder.

For the OPAAB experimental mixtures, identical quantities of raw materials were employed. Nevertheless, differences in the chemical composition of the metakaolin resulted in slight variations in the SiO_2/Al_2O_3 molar ratio between mixtures M1(−R) and M2(+R). In all formulations, the Na_2O/SiO_2 and Na_2O/Al_2O_3 molar ratios were kept constant at 0.2 and 0.6, respectively. The selected SiO_2/Al_2O_3 molar ratios were defined based on the findings of a previous work [36], which demonstrated that higher ratios lead to enhanced mechanical performance.

Mortar produced using the two-part mix (TPM) was adopted as the reference mixture, whose composition was defined according to the mix design proposed by Geraldo et al. [39], which exhibited mechanical properties suitable for civil construction applications.

To produce the mortars, the OPAAB was mixed with sand for 2 min in a mechanical mixer (equipment: Perfecta, São Paulo, São Paulo, Brazil; capacity: 20 L) at slow speed. Thereafter, water was gradually added, and the slurry was mixed for 5 min at medium speed.

The homogenized fresh mix was cast into molds and compacted in a vibrating table for 1 min to eliminate entrapped air. After 3 days, the specimens were demolded, placed into a sealed container exposed at room in laboratory conditions until the date of testing (temperature of 25 ± 2 °C and relative humidity of 60 ± 5%).

2.4. Methods

2.4.1. Air Permeability, Total Water Absorption, and Void Index

- Air permeability

Air permeability of the mortars was determined at 28 days using the Thenoz method, as presented by Geraldo et al. [39]. For the test, cylindrical specimens (50 mm in diameter and 100 mm in height) were molded and cured in laboratory conditions for 25 days (average temperature of 25 ± 2 °C and relative humidity of 60 ± 5%). After curing, the cylindrical specimens were cut into three parts, and the central slice (50 mm in height) was oven-dried (60 ± 2 °C) for 48 h. After cooling, they had their lateral surfaces sealed to guarantee that the flow was uniaxial and perpendicular to the cross-sectional area. The average

values of three specimens of each mortar composition were reported. Air permeability was calculated by Equation (1), which is based on Darcy's law.

$$k = [\mu \cdot s \cdot 1/(\rho \cdot g \cdot t \cdot S)] \cdot \ln(h_0/h_1), \quad (1)$$

where k = air permeability coefficient (m^2); μ = air viscosity at the test temperature (Pa s); ρ = density of water (kg/m^3); g = gravity acceleration (m/s^2); S = cross-sectional area of the sample (m^2); s = cross-sectional area of the capillary tube (m^2); h_0 = starting water level (m); h_1 = final water level (m); 1 = sample height (m); and t = testing time (s) (time for water to pass from h_0 to h_1).

- Total water absorption and void index

The total water absorption and void index were determined in accordance with NBR 9778 [40]. For the tests, cubic specimens (40 mm × 40 mm × 40 mm) were molded and cured in laboratory conditions (temperature of 25 ± 5 °C) for 25 days. Then, the specimens were oven-dried for 48 h (temperature of 60 ± 2 °C) and weighed (dry weight—W_{Dry}). Thereafter, the specimens were immersed in water for 24 h and weighed using a hydrostatic scale (immersed weight—W_{Im}). The saturated weight (W_{Sat}) was obtained by removing excess water from the specimen surfaces with a cloth and weighing. The results were calculated by Equation (2) (water absorption) and Equation (3) (void index).

$$Wa = [(W_{Sat} - W_{Dry})/W_{Dry}] \cdot 100, \quad (2)$$

$$Vo = [(W_{Sat} - W_{Dry})/(W_{Sat} - W_{Im})] \cdot 100, \quad (3)$$

where Wa = water absorption (%); Vo = void index (%); W_{Sat} = specimen saturated mass after immersion (kg); W_{Dry} = specimen oven-dried mass (kg); and W_{Im} = specimen immersed mass (kg).

2.4.2. Resistance to High Temperature

This test was carried out to evaluate the OPAAB performance in a fire situation or other forms of exposure to high temperatures. For each mortar, 3 cubic specimens (40 mm × 40 mm × 40 mm) were molded and cured in laboratory conditions (average temperature = 25 ± 5 °C and RH = 60 ± 5%) for 26 days, when they were dried for 48h in an oven at a temperature of 60 °C. Next, the samples were placed in a muffle furnace (Quimis Aparelhos Científicos Ltd. (Diadema, São Paulo, Brazil); maximum temperature: 1200 °C) and subjected to heat. The average heating rate used was 25 °C/min, and the specimens were kept at 900 °C for 1 h.

Relative mass loss and residual compressive strength after exposure to high temperature were evaluated. To verify the residual mass loss, each specimen had its mass recorded before and after the exposure to high temperature). The final mass was obtained after cooling at room temperature. The test of compressive strength was conducted immediately after the specimens were weighed (Versa Tester machine, Solotest, São Paulo, São Paulo, Brazil; capacity: 150 kN). Mortars cured in laboratory conditions, and tested at the same age, were used as reference.

2.4.3. Resistance to Wet–Dry Cycles

The mortars were subjected to wet–dry cycles to evaluate their mechanical performance in an accelerated aging process at early ages.

For the test, cubic specimens (40 mm × 40 mm × 40 mm) were molded, demolded after 72 h, and immediately subjected to the wet–dry cycle. A total of three specimens

of each mortar mix were produced, and their results were compared to mortars cured in laboratory conditions (average temperature = 25 ± 5 °C and RH = 60 ± 5%).

The wet–dry cycle proposed consisted of four distinct stages: (1) air drying (temperature of 25 ± 5 °C); (2) total water immersion; (3) air drying (temperature of 25 ± 5 °C); and (4) oven drying (temperature of 60 ± 2 °C). The steps and oven temperature were defined and followed sequentially based on what was presented by Farias Filho et al. [41], with modifications in the total duration of each step. Figure 1 provides a visual representation of the time allocated for each of these sequential steps.

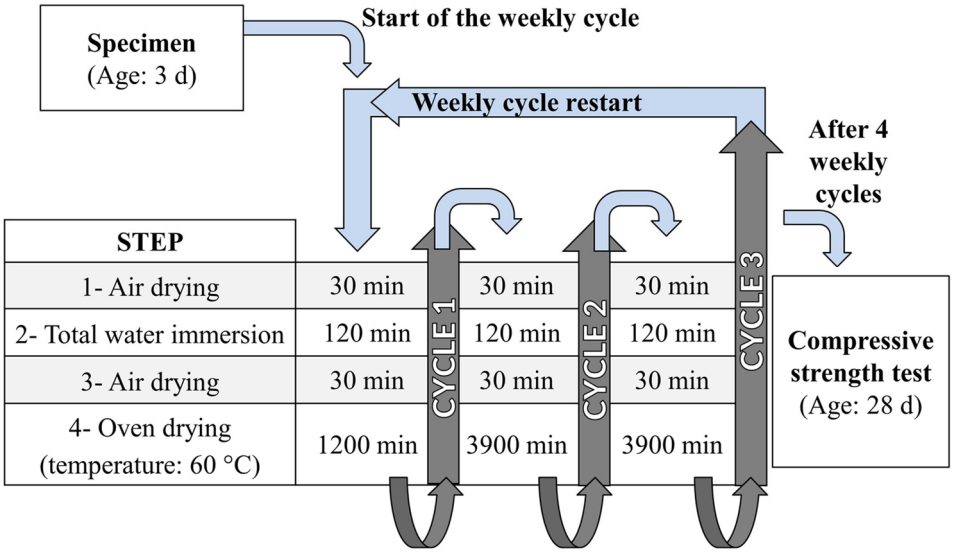


Figure 1. Details of the wet–dry cycles.

After 28 days, with the specimens passing 4 times through each of the cycles (a total of 12 cycles), the specimens were removed from the oven to cool in laboratory conditions. Subsequently, the specimens were tested (the compressive strength) in a Versa Tester machine with a capacity of 150 kN.

2.4.4. Sulfate and Acid Attack

External acid and sulfate attack was evaluated using the method detailed below, which was based on the procedure described by Aiken et al. [42].

Cylindrical specimens (50 mm in diameter and 100 mm in height) were molded and kept in laboratory conditions (average temperature of 25 ± 5 °C) for 24 days, and then they were oven-dried at temperature of 50 °C for 48 h. At 26 days, the dry mass of the specimens was measured, and then they were immersed in tap water to saturate the pores before the test, as described by Sturm et al. [43], remaining in this condition for 48 h.

At 28 days, some of the specimens were immersed in a sulfuric acid solution (5% mass concentration; measured pH ≤ 0.05), while other specimens were immersed in a magnesium sulfate heptahydrate solution (5% mass concentration; pH = 6.32), and other specimens in tap water (used as reference). In each type of immersion, 3 specimens of each sample were used. The sulfuric acid and magnesium sulfate heptahydrate concentrations were selected based on the most aggressive scenario tested by Aiken et al. [42], who employed a 5% solution to investigate the resistance of alkali-activated binders under accelerated acidic attack conditions. The resulting pH of sulfuric acid solution was lower than 1, representing a more severe environment than that adopted by Sturm et al. [43]. The test of resistance to sulfate attack was made with magnesium sulfate heptahydrate due to its availability and high solubility in water.

After weighing the appropriate proportions of reagent and distilled water at the concentrations used (5% by mass), the solutions were mixed by stirring until the complete dissolution of each reagent. Subsequently, the solutions were poured separately into plastic containers containing the identified specimens, which remained immersed in the aggressive environments for a total period of 56 days. The plastic containers remained covered during the test period. After 28 days of immersion, the solutions were changed to renew the aggressive environment.

The masses of the specimens (saturated surface-dry) were measured after 0, 3, 7, 14, 21 28, 35, 42, 49, 52, and 56 days of immersion in the sulfate and acid solutions to verify the mass variation as a function of the time of exposure. At the end of the 56 days, the specimens were kept for 6 h at room temperature (temperature of 25 ± 5 °C) and oven-dried (temperature of 50 °C for 48 h). At the end of the drying cycle, a compressive strength test was conducted (Versa Tester machine; capacity: 150 kN), and the respective loss of compressive strength after the chemical attack cycle was verified. Considering the total time interval resulting from molding the specimens and conducting the procedure described, the compressive strength of the specimens subjected to acid or sulfate attack was obtained after 86 days.

3. Results and Discussion

Figure 2 shows the results for air permeability, total water absorption, and void content.

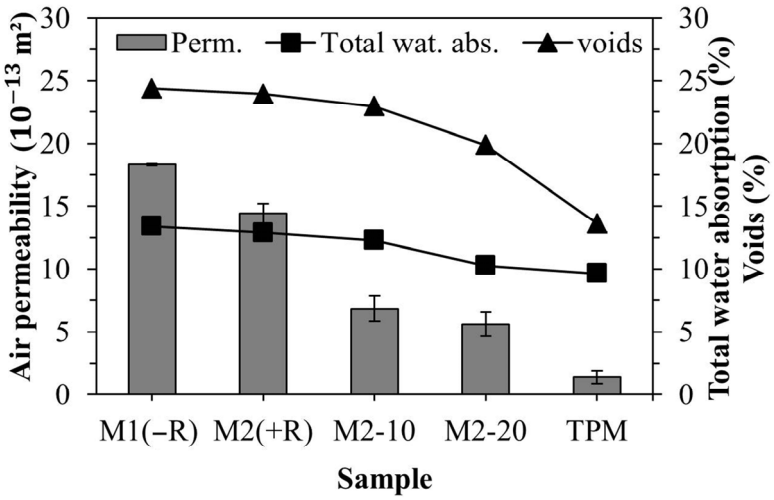


Figure 2. Results of air permeability, total water absorption, and voids of the mortars.

The type of metakaolin and the water content used in the mixture had a marked effect on the results of air permeability, total water absorption, and void index of mortars. M2(+R) exhibited lower porosity and permeability compared to M1(−R), which is related to the use of a more reactive precursor. The high reactivity of the precursor results in a denser matrix with lower porosity [44].

It is important to note that M2(+R) had a consistency index almost 75% higher than M1(−R) [37]. The higher fluidity of M2(+R), when compared with M1(−R), facilitated specimen molding, decreasing the trapped air content in the hardened state.

As expected, the reduction in water content to produce the mortar resulted in lower porosity. The higher the amount of water used in production, the higher the number of voids in solid material. As explained by Provis et al. [45], unlike PC-based products, in AAB, the water does not react, chemically decreasing the porosity. Therefore, the water content used in the production of the mortar is totally related to the final porosity. Higher water contents result in products containing a high number of large pores [46]. These pores

are pathways for the internal movement of aggressive agents and for the leaching of the free alkali, which can result in efflorescence [47].

The results indicate that the use of more reactive metakaolin and the decrease in the water content of the mixture resulted in lower porosity and permeability. The mortars produced with OPAAB were more permeable than TPM mortars (Figure 2). The air permeability of sample M1(−R) was almost 13 times higher than TPM, a mortar made with similar materials, but with a two-part mixing method [39]. The higher permeability observed in OPAAB may be attributed to differences in microstructural development between one-part and two-part alkali-activated systems. The proportion of macropores in OPAAB is higher than TPM mortars (Figure 2), which also corresponds to the high values of permeability, water absorption, and voids. Higher permeability has important implications for durability, as it enhances the transport rate of deleterious agents into the material's interior.

Figure 3 shows visual aspects of the mortars cured in air, submitted to the wet–dry cycle, and after the high-temperature cycle.

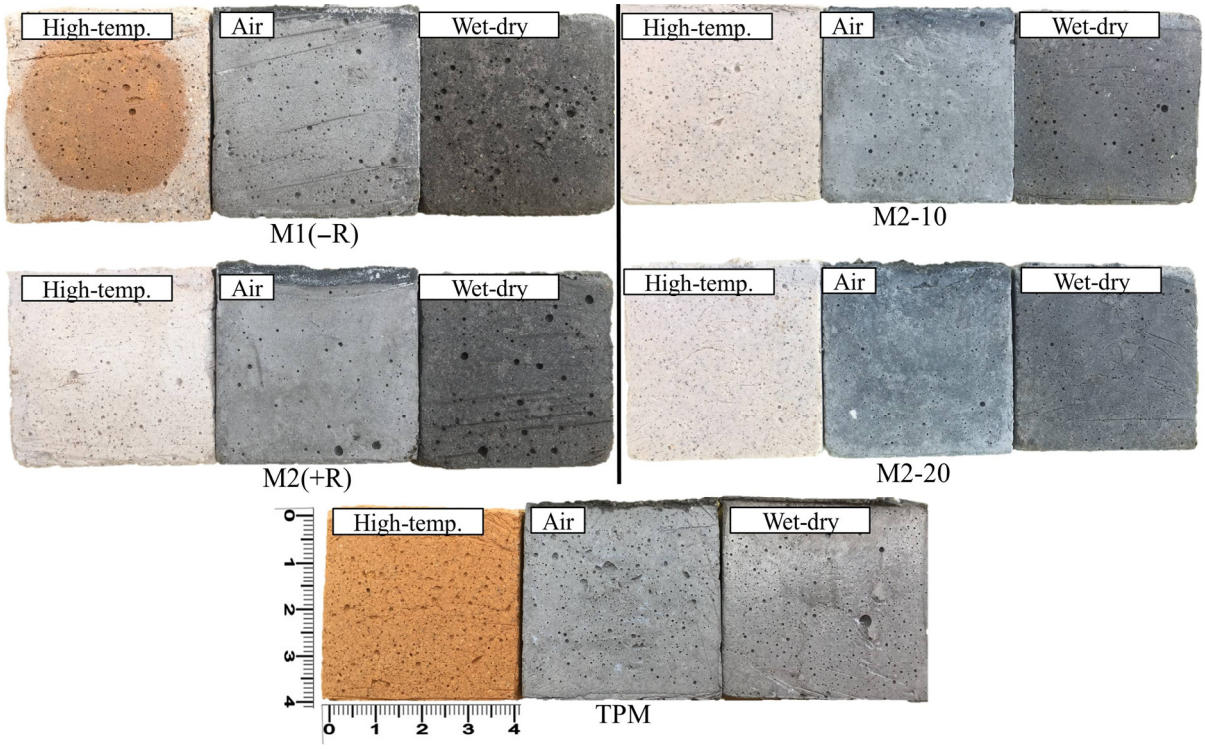


Figure 3. Visual aspects of the mortars cured in air, submitted to the wet–dry cycle, and after the high-temperature cycle.

All tested samples maintained their structural integrity after the heat exposure. A visual inspection revealed that the mortars cured under wet–dry cycles acquired a darker color compared to the samples cured under ambient conditions, which was more pronounced in OPAAB than in TPM.

After exposure to heat, the materials lost their dark color. M1(−R) and TPM were slightly darker than M2(+R), which is attributed to the inherent color of the metakaolin used as a precursor.

The central part of M1(−R) formed darker coloration than that observed in the surface region. This fact may indicate differences in the maximum temperatures reached by each region of the sample (central and superficial). According to Kong and Sanjayan [48], the specimen size influences temperature distribution. If the temperature is significantly

different, it favors thermal shrinkage cracking. All samples showed the appearance of small cracks on the surface and some shrinkage after heat exposure.

Figure 4A shows the compressive strength results of mortars made with different metakaolin and cured in air, subjected to wet–dry cycles or at high-temperature (900 °C). Figure 4B indicates the relative loss of mass and compressive strength of the mortars after high-temperature exposure.

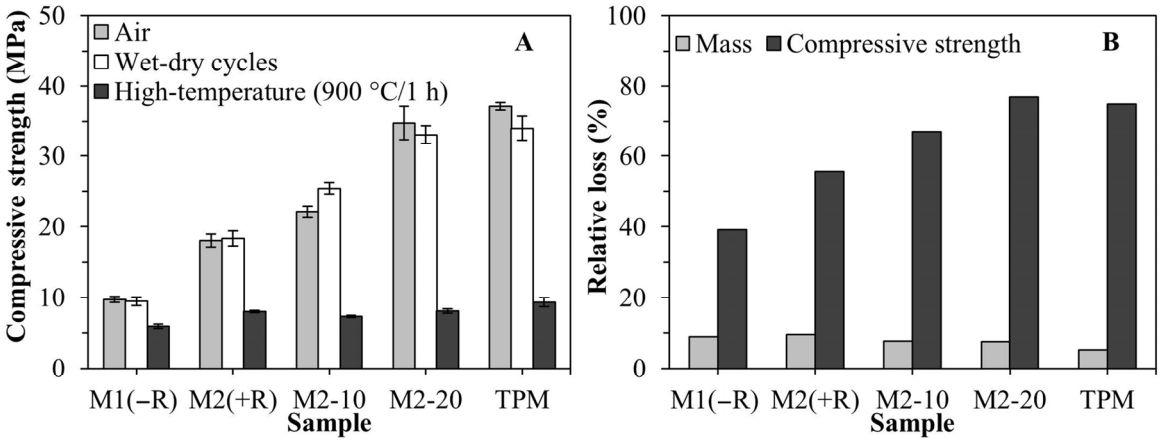


Figure 4. Results of compressive strength of mortars cured in air, subjected to wet–dry cycles, and exposed to high temperature (**A**); relative mass and compressive strength loss after heat exposure (**B**).

Mortars had a decrease in compressive strength after exposure to high temperature. In all OPAAB blends, higher initial mechanical strength was associated with lower mass loss and higher loss of compressive strength. TPM had the lowest mass loss, but it had the second highest relative loss of compressive strength, surpassed only by M2-20.

The increase in temperature stimulates water vaporization resulting from the loss of chemically bound water. This process increases the pore pressure, causing saturation of the pores present in the mortar. The growth of internal pressure in the pore network leads to microcrack formation, which affects the mechanical properties [49].

All OPAAB-based mortars showed residual values of compressive strength higher than 5 MPa after high-temperature exposition.

M2(+R), M2-10, and M2-20 had a decrease in compressive strength after heat exposure of about 55%, 67%, and 76%, respectively. The data indicate that the initial water content played a significant role, with lower water content correlating with higher relative compressive strength loss.

In the literature, Kong and Sanjayan [48] stated that AAB materials can have better performance compared to PC products when exposed to high temperatures. The low performance of PC products, when subjected to excessive heat, is attributed to the decomposition reaction of the hydrated lime present in the material (from 400 °C), which contributes to a decrease in mechanical strength, often causing product decay. Alkali-activated mortars made with a two-part mix also presented a decrease in compressive strength when submitted to high temperatures [50].

The results for mortars subjected to wet–drying cycles revealed that the adopted procedures did not affect the development of compressive strength, as the values were comparable to those obtained for mortars with the same mixture proportions cured under air conditions for an equivalent period.

Figure 5 reveals the visual aspects of the mixtures after the immersion tests in sulfate (Figure 5a) and acid (Figure 5b).

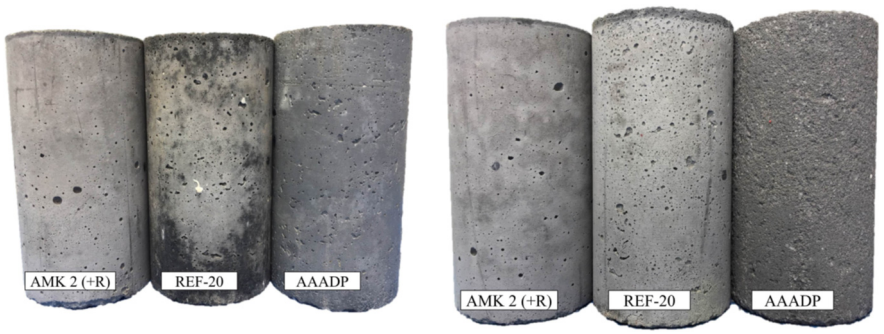


Figure 5. Visual aspects of mortars after 56 days of exposure to 5% sulfate (**a**) and 5% sulfuric acid (**b**).

Figure 6 shows the relative mass changes after sulfate and acid attack as a function of time.

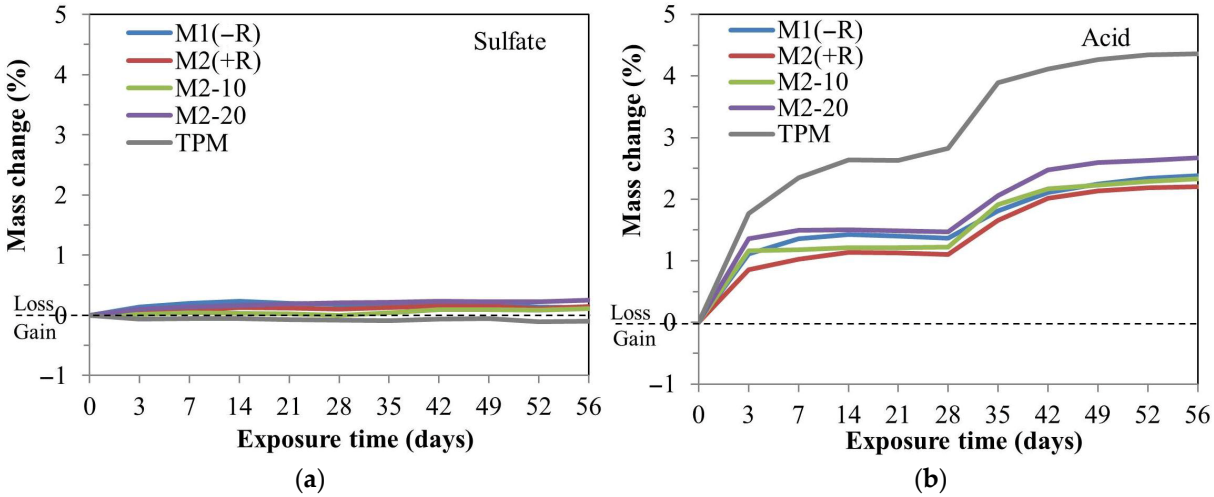


Figure 6. Results of mass changes in mortars over 56 days of exposure to (**a**) 5% sulfate and (**b**) 5% sulfuric acid.

The sulfate attack resulted in a slight mass gain in the TPM. OPAAB-based mixtures showed similar results, with a low relative mass loss over time.

All the mortars lost mass during the acid attack, but TPM had a more significant decrease than the other samples. MK2-20 had the highest relative mass loss. After 56 days, TPM lost almost twice as much mass as MK2(+R).

The acid attack on the internal aluminosilicate structure resulted in the removal of Al, breaking the Si-O-Al chemical bonds. This process increased the presence of Si-OH and Al-OH groups in the solution, resulting in mass loss of AAB-based product [51]. A slight mass gain was observed in samples made with OPAAB from 21 to 28 days, suggesting the potential formation of additional compounds in the AAB during the attack period [42].

Sata et al. [52] reported that PC-based mortars subjected to a sulfuric acid solution (3% concentration) for 120 days had much more significant surface deterioration and mass loss than AAB mortars under similar conditions.

During the initial 7 days and at 35 days, more significant mass losses were found. In subsequent periods, mass loss still occurred, but more gradually. This phenomenon is related to the alkaline nature of the samples, leading to an increase in pH that gradually reduces the aggressiveness of the environment. The average pH values obtained in the acid and sulfate solution containing the samples after 28 days were 2.3 and 8.8, respectively, confirming a certain alteration in the characteristics of the environment over

time. This pH increase is related to the dissolution of the compounds present in the AAB caused by the acid and sulfate, releasing some compounds such as sodium and silicon into the solution [43,53].

The increase in pH observed over the test period certainly reduced the potential for mortar degradation caused by aggressive solutions. However, from a practical perspective, exposure scenarios, such as acid rain, are transient and do not subject mortars to prolonged acid contact. For instance, rain is already considered strongly acidic when the pH is below 4.5 [54]. This value is relatively high even for the pH measured after 28 days of immersion.

Figure 7A shows the compressive strength of the mortars immersed in water (reference) and in aggressive environments (sulfate and acid solutions). Figure 7B shows the relative variation in the compressive strength of the specimens. The mortars were 86 days old at the time of the test.

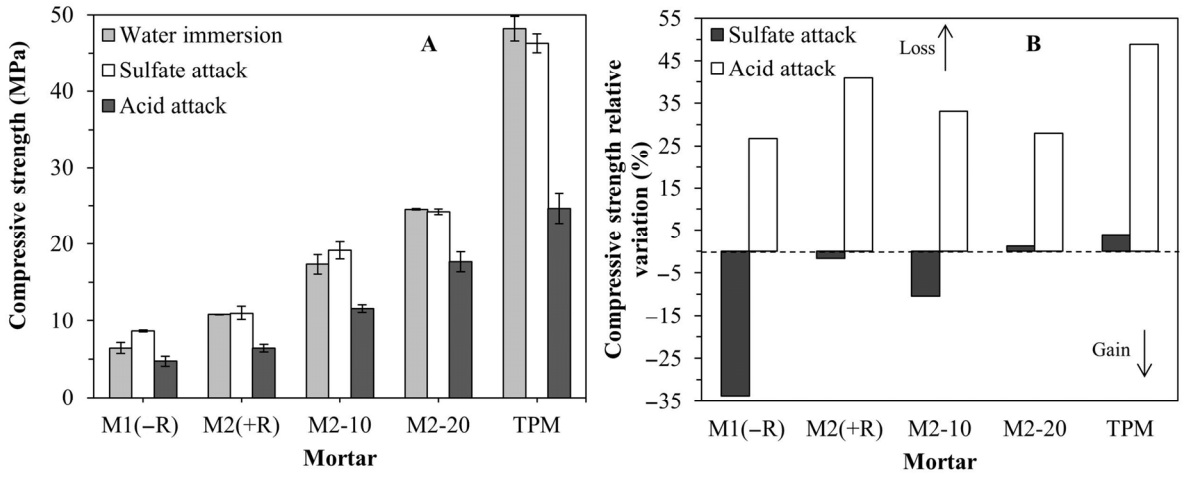


Figure 7. Compressive strength after 56 days of exposure to water, 5% sulfate, and 5% sulfuric acid (**A**); relative variation in compressive strength (**B**).

The compressive strength increased in M1(−R), M2(+R), and M2-10 after the sulfate attack compared to the specimens immersed in water. M1(−R) had a compressive strength increase of 33%. In this same sulfate-rich environment, both M2-20 and TPM had minimal compressive strength losses (less than 4% when compared to specimens immersed in water). The data revealed that considering the attack period studied (56 days), the sulfate was not harmful to mortars in terms of mechanical strength.

The mechanisms responsible for mass loss and strength degradation under sulfate and acidic were inferred based on macroscopic observations and durability performance. However, the absence of microstructural analyses represents a limitation of the present study.

In the literature, Dzunuzovic et al. [53] also reported a high resistance of a two-part mix AAB to external sulfate attack even considering a longer period of exposure (180 days), and the performance depended on the composition of the binder. Sata et al. [52] stated that AAB can develop higher resistance to sulfate attack compared to PC. This occurs because, over time, sulfate exposure in PC mortars leads to the formation of expansive products like ettringite and gypsum ($CaSO_4 \cdot 2H_2O$), inducing internal stresses and subsequent cracking. In contrast, AAB mortars showed minimal dimensional variation, even after 360 days of immersion in a sodium sulfate solution with a concentration of 5% [52].

As the samples produced with the OPAAB proposed in the present research had low calcium content, an attack mechanism different from that observed in PC was expected. The extensive range of precursor materials and dosages present in the literature makes it difficult to understand the exact mechanism of sulfate attack on the matrix [55].

All the mortars lost compressive strength after the acid attack. The compressive strength decreases for M2(+R), M2-10, and M2-20 were 40%, 33%, and 27%, respectively.

The data indicate that the water content of mixing influenced the decrease in the mechanical strength of the sample. The water content directly influenced the final porosity of the specimen, with higher contents resulting in increased porosity. The presence of pores facilitated the penetration of sulfuric acid into the sample, resulting in faster degradation [43].

Despite presenting lower permeability and porosity, TPM mortars showed greater degradation under sulfuric acid exposure. This apparent discrepancy suggests that durability under acidic environments is not governed solely by total permeability, but also by the chemical stability of the binder matrix. Even in systems with lower overall porosity, interconnected pores may facilitate acid ingress, while specific characteristics of the two-part alkali-activated binder may render its surface more susceptible to acid-induced dissolution when compared to one-part systems.

The residual compressive strength of M1(−R) and M2(+R) after acid attack was lower than that obtained after the high-temperature test. For all other specimens tested, the compressive strength results after exposure to high temperature were lower than those after acid attack, indicating that the high temperature caused more significant damage.

All the mortars lost more than 25% in compressive strength after the sulfuric acid attack. This fact has been reported in studies on the durability of AAB and PC [42,43,56]. Despite the reduction in compressive strength, all the specimens remained intact after the test, with a residual compressive strength exceeding 4 MPa.

In the literature, previous studies indicate that AAB usually has a higher resistance to acid attack than PC under the same conditions. The deterioration of binders in an acid environment involves ionic exchange reactions that lead to the decomposition of hydrated and anhydrous compounds (breaking of the nano and microstructure) present in the hardened product, leading to weakening of the material [55,57,58].

Aiken et al. [42] reported strength losses after immersion in sulfuric acid (concentration: 5%, period: 56 days), ranging from 61% to 67% in two-part AAB-based mortars and 74% in PC-based mortars.

In the present work, the loss of compressive strength after immersion in acid varied between 26% and 40% for OPAAB-based mortars and 48% for TPM. Sturm et al. [43] showed that OPAAB-based mortars performed satisfactorily when exposed to sulfuric acid, meeting the requirements of a European technical standard.

Aiken et al. [42] summarized the mechanism of sulfuric acid attack on the AAB matrix in four steps: (1) ion exchange with sodium transfers to the acidic solution (which causes an increase in the pH of the solution) of H^+, H3O$^+$, and $SO_4{}^{2-}$; (2) the hydrogen protons (H^+, H_3O^+) attack the Si-O-Al bonds, resulting in the release of aluminum; (3) other elements can also be transferred in the acid solution (calcium, iron, and magnesium, for example); (4) diffuse $SO_4{}^{2-}$ anions combine with the calcium present in the sample, forming gypsum, which is expansive. However, gypsum formation is low in AAB with low calcium content. In AAB made with low calcium content, acid attack leads to the leaching of Al and Na present in the AAB structure, which increases the SiO_2/Al_2O^3 molar ratio [52,55].

4. Conclusions

In this paper, the durability performance of mortars made with one-part alkali-activated binder (OPAAB) incorporating an alternative sodium silicate derived from rice husk ash was systematically evaluated and compared with a two-part alkali-activated binder (TPM) produced using the same precursors. The following conclusions can be drawn.

- The decrease in the water content used to produce the mortars led to reductions in the porosity and permeability of the materials. The OPAAB-based mortars presented higher porosity compared to mortar made in a two-part mixture, indicating microstructural differences between the one-part and two-part alkali-activated systems.
- The wet–dry cycles applied to mortars only 3 days after molding did not result in compressive strength reduction, resulting only in minor surface discoloration. This suggests that the OPAAB produced can develop a good performance when submitted to wet–dry cycles.
- The OPAAB-based mortars remained structurally intact after exposure to high temperature (temperature of 900 °C for 1 h). All specimens maintained a residual compressive strength higher than 5 MPa after the test, which is very important in fire situations.
- Exposure to sulfate-rich environments (concentration of 5% by mass for 56 days) caused negligible mass variation and no significant loss of compressive strength, indicating good sulfate resistance for both OPAAB and TPM mortars over the evaluated period.
- The immersion of specimens in acid solution (concentration of 5% by mass for 56 days) demonstrated that TPM mortars lost proportionally more mass and compressive strength than the OPAAB-based mortars. All the mortars made with the OPAAB had a residual compressive strength higher than 4 MPa.

The findings are very relevant, suggesting that the OPAAB proposed, in addition to its environmental benefits, favors production and commercialization and can develop good performance in aggressive environments. The results indicate that OPAAB incorporating an alternative sodium silicate derived from rice husk ash may provide improved durability, which is an essential property for product development and application in the construction field, as it indicates an increase in service life. Future research should focus on advancing the microstructural understanding of degradation mechanisms, optimizing mixture design parameters, and assessing long-term performance.

Author Contributions: Conceptualization, G.C. and R.H.G.; methodology, G.C. and R.H.G.; validation, G.C., J.P.G., and R.H.G.; formal analysis, G.C., J.P.G., and R.H.G.; investigation, G.C. and R.H.G.; resources, G.C. and R.H.G.; data curation, G.C., J.P.G., and R.H.G.; writing—original draft preparation, R.H.G.; writing—review and editing, G.C., J.P.G., and R.H.G.; visualization, G.C., J.P.G., and R.H.G.; supervision, G.C.; project administration, G.C.; funding acquisition, G.C. All authors have read and agreed to the published version of the manuscript.

Funding: The authors gratefully acknowledge the financial support provided by the National Council for Scientific and Technological Development (CNPq) and by the Coordenação de Aperfeiçoamento de Pessoal de Nível Superior—Brasil (CAPES)—Finance Code 001.

Data Availability Statement: The original contributions presented in this study are included in the article. Further inquiries can be directed to the corresponding author.

Conflicts of Interest: The authors declare no conflicts of interest.

Abbreviations

The following abbreviations are used in this manuscript:

OPAAB	One-part alkali-activated binder
AAB	Alkali-activated binder
PC	Portland cement
GHG	Greenhouse gas
CO_2	Carbon dioxide
RHA	Rice husk ash

NaOH	Sodium hydroxide
MK	Metakaolin
TPM	Two-part mix
ASSP	Alternative sodium silicate in powder
RH	Relative humidity

References

1. Rasuli, M.I.; Tajunnisa, Y.; Yamamura, A.; Shigeishi, M. A Consideration on the One-Part Mixing Method of Alkali-Activated Material: Problems of Sodium Silicate Solubility and Quick Setting. *Heliyon* **2022**, *8*, e08783. [CrossRef] [PubMed]
2. Alrefaei, Y.; Dai, J.G. Effects of Delayed Addition of Polycarboxylate Ether on One-Part Alkali-Activated Fly Ash/Slag Pastes: Adsorption, Reaction Kinetics, and Rheology. *Constr. Build. Mater.* **2022**, *323*, 126611. [CrossRef]
3. Davidovits, J. Properties of Geopolymer Cements. In Proceedings of the First International Conference on Alkaline Cements and Concretes, Kiev, Ukraine, 11–14 October 1994; pp. 131–149.
4. Khale, D.; Chaudhary, R. Mechanism of Geopolymerization and Factors Influencing Its Development: A Review. *J. Mater. Sci.* **2007**, *42*, 729–746. [CrossRef]
5. Duxson, P.; Provis, J.L.; Lukey, G.C.; van Deventer, J.S.J. The Role of Inorganic Polymer Technology in the Development of "Green Concrete". *Cem. Concr. Res.* **2007**, *37*, 1590–1597. [CrossRef]
6. Jiang, M.; Chen, X.; Rajabipour, F.; Hendrickson, C.T. Comparative Life Cycle Assessment of Conventional, Glass Powder, and Alkali-Activated Slag Concrete and Mortar. *J. Infrastruct. Syst.* **2014**, *20*, 04014020. [CrossRef]
7. Robayo-Salazar, R.A.; Mejía-Arcila, J.M.; Mejía de Gutiérrez, R. Eco-Efficient Alkali-Activated Cement Based on Red Clay Brick Wastes Suitable for the Manufacturing of Building Materials. *J. Clean. Prod.* **2017**, *166*, 242–252. [CrossRef]
8. Borges, P.H.R.; Lourenço, T.M.D.F.; Foureaux, A.F.S.; Pacheco, L.S. Estudo Comparativo Da Análise de Ciclo de Vida de Concretos Geopoliméricos e de Concretos à Base de Cimento Portland Composto (CP II). *Ambiente Construído* **2014**, *14*, 153–168. [CrossRef]
9. Weil, M.; Dombrowski, K.; Buchwald, A. Life-Cycle Analysis of Geopolymers. In *Geopolymers: Structure, Processing, Properties and Industrial Applications*; Provis, J., van Deventer, J.S.J., Eds.; Woodhead Publishing Limited: Cambridge, UK, 2009; pp. 194–210. ISBN 978-1-84569-449-4.
10. Mellado, A.; Catalán, C.; Bouzón, N.; Borrachero, M.V.; Monzó, J.M.; Payá, J. Carbon Footprint of Geopolymeric Mortar: Study of the Contribution of the Alkaline Activating Solution and Assessment of an Alternative Route. *RSC Adv.* **2014**, *4*, 23846–23852. [CrossRef]
11. Abdulkareem, M.; Havukainen, J.; Nuortila-Jokinen, J.; Horttanainen, M. Environmental and Economic Perspective of Waste-Derived Activators on Alkali-Activated Mortars. *J. Clean. Prod.* **2021**, *280*, 124651. [CrossRef]
12. Yang, K.H.; Song, J.K.; Song, K. Il Assessment of CO_2 Reduction of Alkali-Activated Concrete. *J. Clean. Prod.* **2013**, *39*, 265–272. [CrossRef]
13. Passuello, A.; Rodríguez, E.D.; Hirt, E.; Longhi, M.; Bernal, S.A.; Provis, J.L.; Kirchheim, A.P. Evaluation of the Potential Improvement in the Environmental Footprint of Geopolymers Using Waste-Derived Activators. *J. Clean. Prod.* **2017**, *166*, 680–689. [CrossRef]
14. Carreño-Gallardo, C.; Tejeda-Ochoa, A.; Perez-Ordonez, O.I.; Ledezma-Sillas, J.E.; Lardizabal-Gutierrez, D.; Prieto-Gomez, C.; Valenzuela-Grado, J.A.; Robles Hernandez, F.C.; Herrera-Ramirez, J.M. In the CO_2 Emission Remediation by Means of Alternative Geopolymers as Substitutes for Cements. *J. Environ. Chem. Eng.* **2018**, *6*, 4878–4884. [CrossRef]
15. Habert, G.; d'Espinose de Lacaillerie, J.B.; Roussel, N. An Environmental Evaluation of Geopolymer Based Concrete Production: Reviewing Current Research Trends. *J. Clean. Prod.* **2011**, *19*, 1229–1238. [CrossRef]
16. McLellan, B.C.; Williams, R.P.; Lay, J.; Van Riessen, A.; Corder, G.D. Costs and Carbon Emissions for Geopolymer Pastes in Comparison to Ordinary Portland Cement. *J. Clean. Prod.* **2011**, *19*, 1080–1090. [CrossRef]
17. Heath, A.; Paine, K.; McManus, M. Minimising the Global Warming Potential of Clay Based Geopolymers. *J. Clean. Prod.* **2014**, *78*, 75–83. [CrossRef]
18. Teh, S.H.; Wiedmann, T.; Castel, A.; de Burgh, J. Hybrid Life Cycle Assessment of Greenhouse Gas Emissions from Cement, Concrete and Geopolymer Concrete in Australia. *J. Clean. Prod.* **2017**, *152*, 312–320. [CrossRef]
19. Nguyen, L.; Moseson, A.J.; Farnam, Y.; Spatari, S. Effects of Composition and Transportation Logistics on Environmental, Energy and Cost Metrics for the Production of Alternative Cementitious Binders. *J. Clean. Prod.* **2018**, *185*, 628–645. [CrossRef]
20. Maddalena, R.; Roberts, J.J.; Hamilton, A. Can Portland Cement Be Replaced by Low-Carbon Alternative Materials? A Study on the Thermal Properties and Carbon Emissions of Innovative Cements. *J. Clean. Prod.* **2018**, *186*, 933–942. [CrossRef]
21. Turner, L.K.; Collins, F.G. Carbon Dioxide Equivalent (CO_2-e) Emissions: A Comparison between Geopolymer and OPC Cement Concrete. *Constr. Build. Mater.* **2013**, *43*, 125–130. [CrossRef]
22. Wang, X.; Wu, W.; Zhang, L.; Fu, L.; Li, X. Preparation of One-Part Alkali-Activated Nickel Slag Binder Using an Optimal Ball Milling Process. *Constr. Build. Mater.* **2022**, *322*, 125902. [CrossRef]

23. Yang, T.; Gao, X.; Zhang, J.; Zhuang, X.; Wang, H.; Zhang, Z. Sulphate Resistance of One-Part Geopolymer Synthesized by Calcium Carbide Residue-Sodium Carbonate-Activation of Slag. *Compos. Part B Eng.* **2022**, *242*, 110024. [CrossRef]
24. Dişçi, E.; Polat, R. The Influence of Nano-CaO and Nano-Al_2O_3 and Curing Conditions on Perlite Based Geopolymer Concrete Produced by the One-Part Mixing Method. *Constr. Build. Mater.* **2022**, *346*, 128484. [CrossRef]
25. Yin, K.; Jiang, Y.; He, H.; Ren, J.; Li, Z. Microstructure and Shrinkage of One-Part Alkali-Activated Slag with Rice Straw Ash. *Constr. Build. Mater.* **2022**, *345*, 128403. [CrossRef]
26. Abdollahnejad, Z.; Luukkonen, T.; Mastali, M.; Giosue, C.; Favoni, O.; Ruello, M.L.; Kinnunen, P.; Illikainen, M. Microstructural Analysis and Strength Development of One-Part Alkali-Activated Slag/Ceramic Binders Under Different Curing Regimes. *Waste Biomass Valorization* **2020**, *11*, 3081–3096. [CrossRef]
27. Shah, S.F.A.; Chen, B.; Oderji, S.Y.; Haque, M.A.; Ahmad, M.R. Improvement of Early Strength of Fly Ash-Slag Based One-Part Alkali Activated Mortar. *Constr. Build. Mater.* **2020**, *246*, 118533. [CrossRef]
28. Guo, S.; Ma, C.; Long, G.; Xie, Y. Cleaner One-Part Geopolymer Prepared by Introducing Fly Ash Sinking Spherical Beads: Properties and Geopolymerization Mechanism. *J. Clean. Prod.* **2019**, *219*, 686–697. [CrossRef]
29. Peng, M.X.; Wang, Z.H.; Shen, S.H.; Xiao, Q.G.; Li, L.J.; Tang, Y.C.; Hu, L.L. Alkali Fusion of Bentonite to Synthesize One-Part Geopolymeric Cements Cured at Elevated Temperature by Comparison with Two-Part Ones. *Constr. Build. Mater.* **2017**, *130*, 103–112. [CrossRef]
30. Askarian, M.; Tao, Z.; Adam, G.; Samali, B. Mechanical Properties of Ambient Cured One-Part Hybrid OPC-Geopolymer Concrete. *Constr. Build. Mater.* **2018**, *186*, 330–337. [CrossRef]
31. Bong, S.H.; Nematollahi, B.; Nazari, A.; Xia, M.; Sanjayan, J. Efficiency of Different Superplasticizers and Retarders on Properties of "one-Part" Fly Ash-Slag Blended Geopolymers with Different Activators. *Materials* **2019**, *12*, 3410. [CrossRef] [PubMed]
32. Lv, W.; Sun, Z.; Su, Z. Study of Seawater Mixed One-Part Alkali Activated GGBFS-Fly Ash. *Cem. Concr. Compos.* **2020**, *106*, 103484. [CrossRef]
33. Abdulkareem, M.; Havukainen, J.; Horttanainen, M. Environmental Assessment of Alkali-Activated Mortars Using Different Activators. In Proceedings of the 17th International Waste Management and Landfill Symposium, Cagliari, Italy, 30 September–4 October 2019.
34. Tong, K.T.; Vinai, R.; Soutsos, M.N. Use of Vietnamese Rice Husk Ash for the Production of Sodium Silicate as the Activator for Alkali-Activated Binders. *J. Clean. Prod.* **2018**, *201*, 272–286. [CrossRef]
35. Villaquirán-Caicedo, M.A.; Mejía De Gutiérrez, R.; Gallego, N.C. A Novel MK-Based Geopolymer Composite Activated with Rice Husk Ash and KOH: Performance at High Temperature. *Mater. Constr.* **2017**, *67*, 117. [CrossRef]
36. Geraldo, R.H.; Gonçalves, J.P.; Camarini, G. Production Process of an Eco-Friendly One-Part Alkali-Activated Binder. *Mater. Res.* **2022**, *25*, e20210433. [CrossRef]
37. Geraldo, R.H.; Gonçalves, J.P.; Camarini, G. Mechanical Properties of an Eco-Friendly One-Part Alkali-Activated Binder: Influence of Metakaolin and Water Content. *Ceram. Int.* **2022**, *49*, 113260. [CrossRef]
38. Provis, J.L. Geopolymers and Other Alkali Activated Materials: Why, How, and What? *Mater. Struct.* **2014**, *47*, 11–25. [CrossRef]
39. Geraldo, R.H.; Fernandes, L.F.R.; Camarini, G. Water Treatment Sludge and Rice Husk Ash to Sustainable Geopolymer Production. *J. Clean. Prod.* **2017**, *149*, 146–155. [CrossRef]
40. *ABNT NBR 9778*; Hardened Mortar and Concrete—Determination of Absorption, Voids and Specific Gravity. Brazilian Association of Technical Standards: Rio de Janeiro, Brazil, 2009; p. 4.
41. Farias Filho, J.; Menezes, R.R.; Ferreira, H.S.; Santana, L.N.L.; Neves, G.A.; Ferreira, H.C. Durability Study of Alternative Mortars Containing Wastes, Estudo Da Durabilidade de Argamassas Alternativas Contendo Resíduos. *Ceramica* **2011**, *57*, 395–403. [CrossRef]
42. Aiken, T.A.; Kwasny, J.; Sha, W.; Soutsos, M.N. Effect of Slag Content and Activator Dosage on the Resistance of Fly Ash Geopolymer Binders to Sulfuric Acid Attack. *Cem. Concr. Res.* **2018**, *111*, 23–40. [CrossRef]
43. Sturm, P.; Gluth, G.J.G.; Jäger, C.; Brouwers, H.J.H.; Kühne, H.C. Sulfuric Acid Resistance of One-Part Alkali-Activated Mortars. *Cem. Concr. Res.* **2018**, *109*, 54–63. [CrossRef]
44. Longhi, M.A.; Zhang, Z.; Rodríguez, E.D.; Kirchheim, A.P.; Wang, H. Efflorescence of Alkali-Activated Cements (Geopolymers) and the Impacts on Material Structures: A Critical Analysis. *Front. Mater.* **2019**, *6*, 89. [CrossRef]
45. Provis, J.L.; Duxson, P.; van Deventer, J.S.J. The Role of Particle Technology in Developing Sustainable Construction Materials. *Adv. Powder Technol.* **2010**, *21*, 2–7. [CrossRef]
46. Hajimohammadi, A.; Provis, J.L.; Van Deventer, J.S.J. One-Part Geopolymer Mixes from Geothermal Silica and Sodium Aluminate. *Ind. Eng. Chem. Res.* **2008**, *47*, 9396–9405. [CrossRef]
47. Zhang, Z.; Provis, J.L.; Reid, A.; Wang, H. Fly Ash-Based Geopolymers: The Relationship between Composition, Pore Structure and Efflorescence. *Cem. Concr. Res.* **2014**, *64*, 30–41. [CrossRef]
48. Kong, D.L.Y.; Sanjayan, J.G. Effect of Elevated Temperatures on Geopolymer Paste, Mortar and Concrete. *Cem. Concr. Res.* **2010**, *40*, 334–339. [CrossRef]

49. Kirchhof, L.D. Estudo Teórico-Experimental Da Influência Do Teor de Umidade No Fenômeno de Spalling Explosivo Em Concretos Expostos a Elevadas Temperaturas. Ph.D. Thesis, Universidade Federal do Rio Grande do Sul, Porto Alegre, Rio Grande do Sul, Brazil, 2010.
50. Chithambaram, S.J.; Kumar, S.; Prasad, M.M. Thermo-Mechanical Characteristics of Geopolymer Mortar. *Constr. Build. Mater.* **2019**, *213*, 100–108. [CrossRef]
51. Bakharev, T. Resistance of Geopolymer Materials to Acid Attack. *Cem. Concr. Res.* **2005**, *35*, 658–670. [CrossRef]
52. Sata, V.; Sathonsaowaphak, A.; Chindaprasirt, P. Resistance of Lignite Bottom Ash Geopolymer Mortar to Sulfate and Sulfuric Acid Attack. *Cem. Concr. Compos.* **2012**, *34*, 700–708. [CrossRef]
53. Džunuzović, N.; Komljenović, M.; Nikolić, V.; Ivanović, T. External Sulfate Attack on Alkali-Activated Fly Ash-Blast Furnace Slag Composite. *Constr. Build. Mater.* **2017**, *157*, 737–747. [CrossRef]
54. Huang, T.; Fan, Y.; Long, Y.; Pang, Z. Quantitative Calculation for the Contribution of Acid Rain to Carbonate Weathering. *J. Hydrol.* **2019**, *568*, 360–371. [CrossRef]
55. Bašcarevic, Z. The Resistance of Alkali-Activated Cement-Based Binders to Chemical Attack. In *Handbook of Alkali-Activated Cements, Mortars and Concretes*; Pacheco-Torgal, F., Ed.; Woodhead Publishing Limited: Cambridge, UK, 2014; pp. 373–393. ISBN 978-1-78242-288-4.
56. Mauri, J.; Dias, D.P.; Cordeiro, G.C.; Dias, A.A. Argamassa Geopolimérica: Estudo Da Degradação Por Sulfato de Sódio e Ácido Sulfúrico. *Rev. Matér.* **2009**, *14*, 1039–1046. [CrossRef]
57. Fernandez-Jimenez, A.; García-Lodeiro, I.; Palomo, A. Durability of Alkali-Activated Fly Ash Cementitious Materials. *J. Mater. Sci.* **2007**, *42*, 3055–3065. [CrossRef]
58. Abora, K.; Beleña, I.; Bernal, S.A.; Dunster, A.; Nixon, P.A.; Provis, J.L.; Arezki, T.-H.; Winnefeld, F. Durability and Testing—Chemical Matrix Degradation Processes. In *Alkali Activated Materials; State-of-the-Art Report, RILEM TC 224-AAM*; Provis, J.L., van Deventer, J.S.J., Eds.; RILEM State-of-the-Art Reports; Springer: Dordrecht, The Netherlands, 2014; Volume 13, ISBN 978-94-007-7671-5.

Disclaimer/Publisher's Note: The statements, opinions and data contained in all publications are solely those of the individual author(s) and contributor(s) and not of MDPI and/or the editor(s). MDPI and/or the editor(s) disclaim responsibility for any injury to people or property resulting from any ideas, methods, instructions or products referred to in the content.